

Synthesis of [¹⁸F]anginex with high specific activity [¹⁸F]fluorobenzaldehyde for targeting angiogenic activity in solid tumors

Scott M. Apana,^a Robert J. Griffin,^b Nathan A. Koonce,^b Jessica S. Webber,^b Ruud P. M. Dings,^c Kevin H. Mayo,^c and Marc S. Berridge^{a,d*}

Anginex is a 33-residue peptide that has been previously demonstrated to possess antiangiogenic properties. To provide a tool to evaluate the regional biodistribution and pharmacokinetics of anginex, and possibly to provide a useful angiogenesis-targeted radiotracer, we have radiolabeled anginex with fluorine-18. High specific activity [¹⁸F]fluorobenzaldehyde (1.5–4.8 TBq (40–130 Ci)/μmol) was used to label anginex via reductive amination in 76% yield. The effective specific activity of the product was lower because unlabeled anginex was not separated. However, the high specific activity labeling reagent increased the labeling yield and reduced the amount of anginex required for labeling. Regional pharmacokinetics were measured by PET scanning in mice, demonstrating tumor uptake and low background, with up to 30% of total injected dose localized in some tumors.

Keywords: fluorine-18; anginex; angiogenesis; tumor imaging; PET

Introduction

Angiogenesis, the growth of new blood vessels from preexisting vessels, is crucial for organ growth as well as organ repair.¹ Angiogenesis plays a key role in normal organ development, but it is also involved in pathological conditions including cancer, arthritis, diabetic retinopathy, and restenosis.^{2–4} Several angiogenesis inhibitors have been approved for use by the US Food and Drug Administration,⁵ and several F-18- and Cu-64- labeled radiotracers are used to image angiogenesis.^{3,6–10} Common endogenous angiogenic inhibitors include angiostatin, platelet factor-4, thrombospondin, interferon-γ inducible protein-10, and endostatin.³

Anginex was designed based on common amino acid sequences of known endogenous inhibitors and has been shown to inhibit endothelial cell growth more effectively than several of these inhibitors.¹¹ Anginex is a synthetic 33-mer peptide with a molecular weight of 3900. The amino acid sequence, using standard single-letter amino acid designations, is H₂N-A-N-I-K-L-S-V-Q-M-K-L-F-K-R-H-L-K-W-K-I-I-V-K-L-N-D-G-R-E-L-S-L-D-C(O)-NH₂.

Note that the compound is a carboxyl-terminal amide.^{4,11} Anginex has been shown to sensitize tumor endothelial cells to radiation,¹² inhibit tumor growth up to 80% in several murine and human tumor models,^{13–15} and may improve tumor response to radiation by improving tumor oxygenation.¹⁶ A lasting influence of anginex therapy on tumor growth inhibition in combination with weekly radiation in a model of focal human multiple myeloma was recently observed.¹⁷

Anginex inhibits tumor growth specifically by binding to galectin-1 (gal-1), which has been found to be overexpressed in endothelial cells of various tumors.¹⁸ By binding to gal-1, anginex disrupts endothelial cell adhesion and migration,

inducing apoptosis and thus inhibiting angiogenesis.¹⁶ Although it is, therefore, an antiangiogenic peptide, it has additional mechanisms of action. The study of inhibition of gal-1 overexpression could lead to the development and use of more effective therapeutic agents.¹⁹ In view of the substantial amount of *in vitro* and *in vivo* evidence that anginex targets the angiogenic microvasculature in tumors and can be a potent adjuvant therapy, we were interested in better understanding the tumor uptake of this peptide *in vivo*.

Anginex radiolabeled with [¹⁸F]fluorobenzaldehyde may permit PET scanning for assessment of regional anginex biodistribution and kinetics. Labeled anginex may thus serve as a tracer to assess angiogenic activity in tumors, which may allow evaluation of optimal radiation therapy scheduling and tumor targeting for therapeutic use of this or other antiangiogenic agents. In preliminary investigations, we obtained substantial tumor localization of labeled anginex in bone grafts of multiple

^a3D Imaging, LLC, Cyclotron Suite Rm PS010, UAMS Radiology #556, 4301 W. Markham Street, Little Rock, AR 72205-7199, USA

^bDepartment of Radiation Oncology, University of Arkansas for Medical Sciences, Little Rock, AR, USA

^cDepartment of Biochemistry, Molecular Biology, and Biophysics, University of Minnesota, Minneapolis, MN, USA

^dDepartment of Radiology, University of Arkansas for Medical Sciences, Little Rock, AR, USA

*Correspondence to: Marc S. Berridge, 3D Imaging, LLC Cyclotron Suite Rm PS010, UAMS Radiology #556, 4301 W. Markham Street, Little Rock, AR 72205-7199, USA. E-mail: MBerridge@3DImagingLLC.com

myeloma¹⁷ as well as in a murine breast tumor model, suggesting that the refinement and expansion of [¹⁸F]anginex may be beneficial for various aspects of oncology. The synthesis of this tracer and the imaging results reported here provide motivation and means to continue to investigate labeled anginex as an antiangiogenic radiotracer for use in tumor research, tumor evaluation, and treatment planning.

Results and discussion

[¹⁸F]Anginex was obtained via reductive amination of high specific activity [¹⁸F]fluorobenzaldehyde with anginex in 76.8 ± 3.5% (*n* = 4) chemical yield (Figure 1). Purification of [¹⁸F]anginex for production was accomplished by C18 cartridge purification rather than HPLC as a matter of preference. Although [¹⁸F]fluorobenzaldehyde can also be retained by C18 cartridge purification, it was conveniently removed during prior solvent evaporations. Neither purification method separated [¹⁸F]anginex from the unlabeled anginex precursor. The effective specific activity of the product therefore depended upon the amount of anginex used in the reaction and was typically about 4 GBq (100 mCi)/mg, or 14.4 GBq (390 mCi)/μmol.

To determine the labeling position of fluorobenzaldehyde, the amounts of both anginex and fluorobenzaldehyde were increased from standard labeling procedure levels and were reacted at 1:1 stoichiometric ratio due to the need for greater detectable mass of the reacted product. Most of the anginex peptide reacted with the labeling reagent, as evidenced by the HPLC results shown in Figure 2. The trace at the bottom is for labeled anginex (using nonradioactive ¹⁹F-fluorobenzaldehyde in this case), whereas the partial trace at the top is labeled anginex spiked with nearly an equimolar amount of standard anginex peptide as indicated. Notice in the bottom HPLC trace of the labeled peptide that apparently less than 1% of free anginex peptide remains from this stoichiometric ratio reaction. These HPLC data also indicate that the conjugation reaction produced three species of labeled anginex in significant amounts—a major one eluting from the HPLC at 63 min (retention time), and two minor ones eluting at 75 and 117 min. Because we used reverse-phase HPLC columns, the hydrophobicity of these species increased with increasing retention time. The labeling reagent could react with any free amine group on the peptide (including 5 lysine ε-amine groups and an N-terminal amine), and the polarity of the peptide product would be reduced as more groups were conjugated. Therefore, the minor, later-eluting products were likely to be multiply substituted.

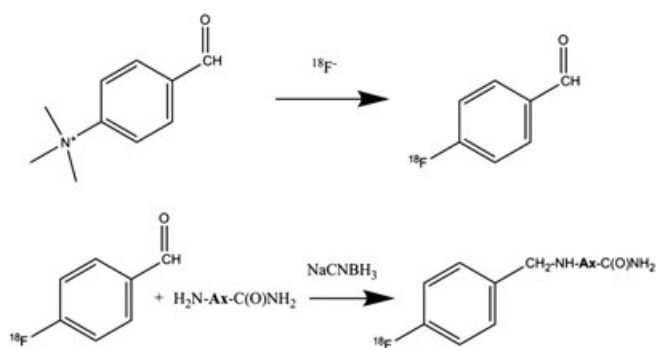


Figure 1. Synthesis of radiolabeled fluorobenzaldehyde and anginex. Ax, anginex 33-mer peptide (see Introduction).

The N-terminal sequencing of anginex proceeded normally through the entire peptide sequence. In contrast, the N-terminal sequencing of any of the reaction products gave no reaction, indicating that the N-terminus is blocked in all products (> 99%), and therefore the N-terminal is the most reactive, preferentially labeled, site in the anginex molecule. This suggests that in this stoichiometric reaction, the N-terminus was labeled first, followed by the reaction of additional sites.

The mass spectral fragmentation patterns of the major (63 min) product suggested that this product was singly substituted. This conclusion was also supported by the lack of observation of the several products that would be expected if multiple reaction sites had similar reactivity, by the N-terminal sequence results, and by the product stoichiometry. In a no-carrier added radiolabeling, anginex is present in excess of the radiolabeled fluorobenzaldehyde. Therefore, the chance of double labeling under labeling conditions is remote. The major product of this reaction is thus the only one of relevance to the radiolabeling conditions, and radiolabeling occurs almost exclusively at the N-terminus.

Concentration dependence

Production batches of [¹⁸F]anginex used the entire 1-mL portion of purified [¹⁸F]fluorobenzaldehyde. This resulted in a 4-fold decrease in the concentration of unlabeled anginex precursor (0.9 vs 4 mg/mL) when 'high' and 'normal' specific activity comparison methods were used. As a result of this difference in concentration, the production batches also saw a corresponding decrease in the yield of [¹⁸F]anginex to 20–30%. Because the overall yield was sufficient, no effort was made to increase the yield of the production batches by either a reduction of the reaction volume or by an increase in the amount of reagents used to a level equivalent with the high specific activity method. The effective specific activity could therefore also be increased, although there was no need to do so for the purpose of this work.

Carrier dependence

Recent work has shown Teflon to be a major source of fluoride carrier in the synthesis of fluorine-18-labeled compounds.²⁰ Prior to the identification of the source of carrier, the average mass of carrier fluoride per synthesis was 400–800 nmol,²⁰ and the corresponding specific activity of many fluorine-18 compounds at multiple centers worldwide was generally 18–111 GBq (0.5–3 Ci)/μmol.^{21–30} By removing all sources of Teflon to reduce the amount of carrier to approximately 25 nmol, with corresponding specific activities of 30–50 Ci/μmol,²⁰ an expected result would be an improvement in yield or a reduction in the amount of precursor needed to maintain a high yield, or both.

To determine whether high specific activity fluorobenzaldehyde improved the overall yield of [¹⁸F]anginex, a comparison was performed by adding carrier fluorobenzaldehyde to adjust the total amount of carrier to an amount that was representative of formerly typical specific activities. This was done prior to addition and reaction of anginex. Whereas the average mass of carrier in fluorine-18 syntheses in prior work was 400–800 nmol,²⁰ the amount of unlabeled fluorobenzaldehyde added as carrier in these experiments was only 250 nmol. This reduction in the added carrier amount was due to the relatively high molecular weight and resulting low molar amount of anginex used for labeling (260 nmol) and a desire to not enter the range

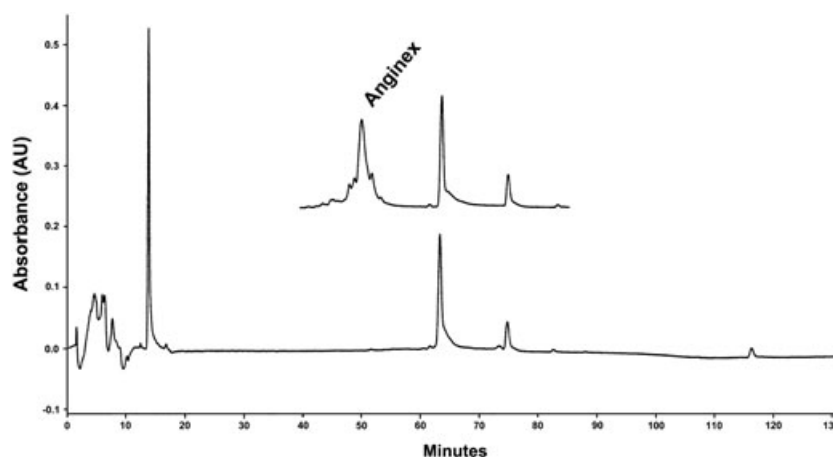


Figure 2. HPLC analysis of the reaction product of fluorobenzaldehyde and anginex (1.1:1). Inset shows the same sample with added unreacted anginex. A singly 'labeled' product eluted at 63 min, and a doubly 'labeled' product eluted at 75 min.

of carrier in which [^{18}F]fluorobenzaldehyde would be in excess over the anginex.

The yield of [^{18}F]anginex in these carrier added syntheses was $58.3 \pm 3.6\%$ ($n=4$), in comparison with a yield of $76 \pm 3.5\%$ without added carrier, indicating a significant increase ($p < 0.05$) in yield with high specific activity fluorobenzaldehyde under otherwise identical conditions.

MicroPET results

An image of a mouse with human BN-myeloma xenograft is shown in Figure 3. The highest organ uptake was observed in liver, with some urinary excretion and residual abdominal cavity activity remaining from the intraperitoneal (i.p.) injection also observed. No other major organs were noted on the image. There was a striking uptake into the dorsal tumor graft, which grew well beyond the normal boundaries of the animal's body (drawn on the figure). Tumor uptake accounted for at most 30% of the total body distribution of labeled anginex and was five times that of muscle background. Maximum tumor uptake was 16% higher than maximal uptake in the liver. We have previously observed that repeated anginex treatment by i.p. injection of 10–20 mg/kg can slightly inhibit SCK (murine mammary carcinoma) and BN myeloma tumor growth and can significantly increase radiation-induced delays in tumor growth in these models.^{12,17} Figure 4 shows tumor uptake in FSall tumor-bearing mice. This tumor, implanted on the hindlimb, accumulated noticeably less anginex than did the BN-myeloma. However, it should also be noted that Figure 4 includes earlier time point image data than Figure 3. Unabsorbed dose from the i.p. injection is more apparent in Figure 4 as an intense abdominal activity than in the image shown in Figure 3, which was acquired at a longer time after injection. Decay-corrected time-activity curves are shown (Figure 5) for tumor and reference muscle regions of interest from the FSall tumor mouse shown in Figure 4. Uptake in tumor from the i.p. injection is slow until a modest maximum after 10 min of about three times the level seen in muscle.

Experimental

Solvents and reagents were purchased from Fisher Scientific and Sigma-Aldrich and were used without further purification unless otherwise noted. Anginex was obtained from the biochemical



Figure 3. Sagittal plane of a 20-min microPET scan of [^{18}F]anginex 2 h after i.p. injection in a SCID-rab BN myeloma tumor-bearing mouse. Arrow indicates the tumor/bone graft, which extends outside the normal body contour (approximate contour indicated by the sketch).

facility of the University of Minnesota as a lyophilized powder and reconstituted in methanol.

HPLC analysis was performed on a Hewlett-Packard 1090 Series II instrument with autoinjector, diode array UV, and a Grace Econosphere $4.6 \times 250\text{ mm}$ reverse-phase column eluted with 40% aqueous acetonitrile/0.2% trifluoroacetic acid at a flow rate of 1.6 mL/min. Retention times (in minutes): [^{18}F]anginex, 3.1; [^{18}F]fluorobenzaldehyde, 6.5. Radioactivity was measured with a Beckman 170 flow-through detector. Radiolabeled anginex co-eluted on this system with unlabeled anginex (precursor).

[^{18}F]-*p*-Fluorobenzaldehyde

Synthesis of [^{18}F]fluorobenzaldehyde was done using previously reported methods.²⁰ Briefly, high specific activity [^{18}F]-fluoride (from 11-MeV proton bombardment of [^{18}O]H₂O) was passed through anion exchange resin, and the [^{18}O]H₂O was recovered. [^{18}F]Fluoride was eluted with aqueous potassium carbonate (24 μmol , 600 μL), Kryptofix 2.2.2 (10 mg, 26 μmol) was added,

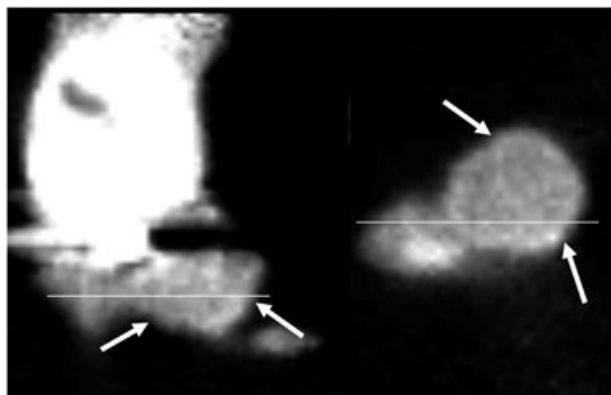


Figure 4. MicroPET image planes of an FSall (mouse fibrosarcoma) tumor on the right hind limb following i.p. injection (left, coronal image slice; right, transaxial image slice). The horizontal line in each image slice shows the approximate position of the plane of the other image slice.

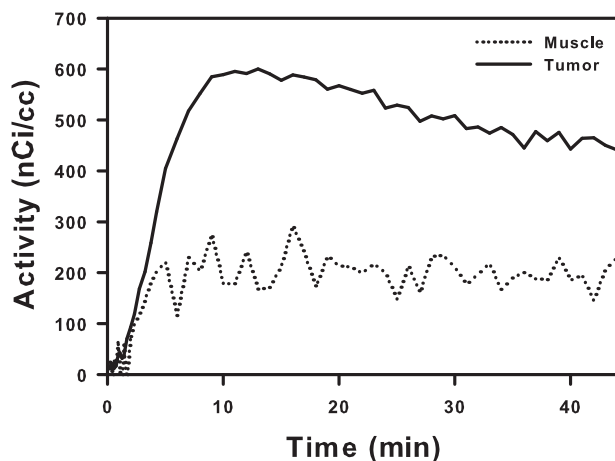


Figure 5. Decay-corrected time-activity curves from the FSall (mouse fibrosarcoma) tumor and corresponding muscle reference region shown in Figure 4.

and [^{18}F]fluoride was dried by acetonitrile evaporation. The precursor *p*-trimethylammoniumbenzaldehyde triflate³¹ (6–8 mg, 19–25 μmol in 1 mL of DMSO) was reacted for 10 min at 100 °C. After C18 cartridge (Waters Sep-Pak) purification and elution with 1 mL of methanol, the labeled fluorobenzaldehyde was used without further purification. Each experiment could be performed with up to 130 GBq (3500 mCi) of [^{18}F]fluoride, depending on the proton beam current and duration used for the experiment. Regardless of the quantity of fluorine-18 produced, however, the mass of fluorobenzaldehyde that was produced in each experiment was in the range of 8–50 nmol.²⁰ Individual experiments were thus performed with fluorobenzaldehyde of measured specific activity in the range of 1.5–4.8 TBq (40–130 Ci)/ μmol .

[^{18}F]Anginex reactions with high specific activity [^{18}F] fluorobenzaldehyde

One milligram of anginex (260 nmol) was dissolved in 100 μL of methanol and added to a portion of the purified [^{18}F]fluorobenzaldehyde solution (50 μL , 0.04–0.8 GBq (1–20 mCi), ~1.25 nmol). To this solution, 4 μL of glacial acetic acid and 100 μg

of sodium cyanoborohydride (1.6 μmol) in 100 μL of methanol were added, and the solution was heated at 100 °C for 30 min. [^{18}F]Anginex was purified by reverse-phase HPLC (Figure 6).

[^{18}F]Anginex reactions with 'normal' specific activity [^{18}F] fluorobenzaldehyde

One milligram of anginex (260 nmol) was dissolved in 100 μL of methanol and added to a portion of the purified [^{18}F]fluorobenzaldehyde solution (50 μL , 0.04–0.8 GBq (1–20 mCi), ~1.25 nmol), to which unlabeled fluorobenzaldehyde (250 nmol) had been previously added. The carrier quantity of 250 nmol had previously been determined to be representative of the amount of carrier present in a typical radiolabeling experiment (400–800 nmol) before improvements in specific activity²⁰ were introduced. To this solution, 4 μL of glacial acetic acid and 100 μg of sodium cyanoborohydride (1.6 μmol) in 100 μL of methanol were added, and the solution was heated at 100 °C for 30 min. [^{18}F]Anginex was purified by reverse-phase HPLC (Figure 6).

[^{18}F]Anginex for imaging use

[^{18}F]fluorobenzaldehyde (16–24 GBq (400–650 mCi), ~25 nmol) in 1 mL of methanol was added to 1 mg of anginex (260 nmol). Glacial acetic acid (4 μL) and 100 μg of sodium cyanoborohydride (1.6 μmol) in 100 μL of methanol were added, and the solution was heated at 100 °C for 30 min. The solvent was evaporated, and the residue dissolved in 10 mL of water. The entire solution was passed over a C18 cartridge (Waters Sep-Pak). The cartridge was rinsed with an additional 5 mL of water and dried briefly with argon. The retained [^{18}F]Anginex was eluted with 1 mL of acetonitrile into a conical glass vial at 100 °C, and the solvent was evaporated under vacuum with argon at a flow rate of 55 mL/min. Ethanol (2 \times 0.5 mL) was added and evaporated to remove acetonitrile. [^{18}F]Anginex was taken up in sterile water, and the pH was adjusted to 6–7 with 1–10 μL of 1 N sodium bicarbonate.

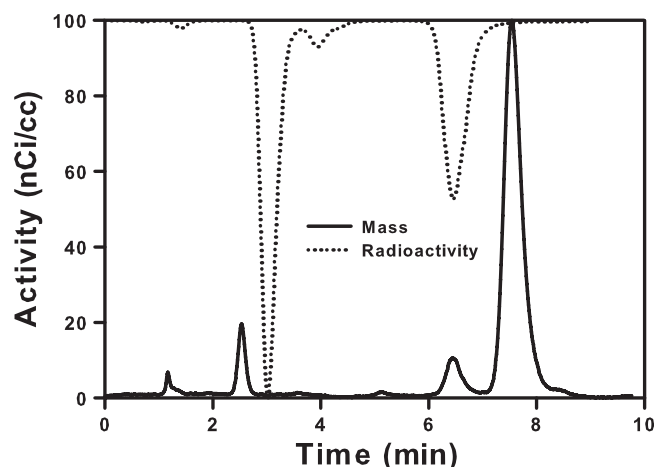


Figure 6. Radiochromatogram of crude anginex following the reaction. Anginex mass in the quantity injected was not detectable. The chromatogram of [^{18}F]Anginex (purified product) consisted of a single mass and the corresponding radioactivity peak and is therefore not shown here.

Fluorobenzyl anginex (^{19}F) and determination of labeling position

Anginex (10mg, 2.6 μmol) was dissolved in 1mL of methanol, and unlabeled fluorobenzaldehyde (2.6 μmol) was added. To this solution, 40 μL of glacial acetic acid and 1mg of sodium cyanoborohydride (16 μmol) in 100 μL of methanol were added, and the solution was heated at 100 $^{\circ}\text{C}$ for 60min. Purification followed the '[^{18}F]anginex for imaging use' method described earlier.

Analysis of the position of labeling of the anginex was performed using an HPLC system capable of separation of analytical quantities of the derivatized anginex products from anginex and from each other. A Beckman Coulter System Gold (125 Solvent Module; 166 Detector) analytical/semi-preparative HPLC with UV detection at 220nm was used, with reverse-phase C18 Kromasil columns and an elution gradient of 0% to 60% acetonitrile with 0.1% trifluoroacetic acid in water. Fractions from the HPLC were collected for analysis of m/z on a MALDI-TOF mass spectrometer (4800 MALDI TOF/TOF, Applied Biosystems). Fractions were also analyzed by N-terminal sequencing via Edman degradation in a Beckman 1600N-terminal sequencer. Authentic, underivatized anginex was also added to the sample for positive chromatographic identification of the unreacted and reacted materials.

Tumors and animals

All experimental methods were approved by the Institutional Animal Care and Use Committee at the University of Arkansas for Medical Sciences (UAMS). Animals were housed in a temperature-controlled environment (72 \pm 2 $^{\circ}\text{F}$) with a 12-h light cycle and were fed with a commercially prepared diet (Harlan, Indianapolis, IN) and provided water *ad libitum*. Mice were subjected to imaging analysis using UAMS microPET Focus 220 (Concorde Microsystems, Knoxville, TN) when the tumors grew to 8–12mm in size.

Human BN myeloma

In vitro expansion of the BN cells was performed as previously described.³² Briefly, mononucleated marrow cells from human fetal long bones (Advanced Bioscience Resources, Alameda, CA) were used as feeder cells and cultured in flasks in low-glucose DMEM supplemented with 10% fetal bovine serum (Hyclone, Logan, UT) and antibiotics. SCID-rab mice were prepared as previously described.³³ Briefly, rudiments of long bones of newborn New Zealand rabbits (Myrtle Rabbitry, Thompson Station, TN) were implanted s.c. in 6-week-old CB.17/lcr-SCID mice (Harlan Sprague Dawley, Indianapolis, IN). Six to eight weeks after implantation of the bone grafts, BN cells (0.5 \times 10⁶–2 \times 10⁶ cells in 50–100 μL of PBS) were injected directly into the marrow cavity of the implanted bone grafts through the diaphyseal opening. Mice were imaged after tumor growth extended outside the graft. For imaging, mice were anesthetized in an induction chamber with 4–5% isoflurane in oxygen and maintained at 1.5–2.5% isoflurane in oxygen during the scan.

Mouse fibrosarcoma—FSall

FSall cells, mouse fibrosarcoma, were cultured in RPMI 1640 medium (Mediatech Inc., Manassas, VA) supplemented with 10% bovine calf serum (Hyclone Laboratories Inc., Logan, UT).

Cells were harvested in log phase with 0.125% trypsin (Mediatech Inc.), counted with a Z2 Coulter Counter (Beckman Coulter, Brea, CA), spun, and resuspended in serum-free medium at a concentration of 2 \times 10⁵ cells/50mL. Female C3H mice were purchased from Charles Rivers (Wilmington, MA), and tumor cells were injected s.c. in the right hind limb. Mice were imaged when tumors grew to 8–10mm in size.

MicroPET—BN myeloma

Static microPET imaging was performed on three BN myeloma tumor graft-bearing mice at 2h after i.p. injection with 1.1MBq (30 μCi) of [^{18}F]anginex tracer in a solution of 10mg/mL unlabeled anginex. Static scans through the tumor region were captured for 20min, and a two-dimensional OSEM image reconstruction was used. Decay-corrected images were used to draw regions of interest around the BN tumor and whole body (Figure 3). Activities within the tumor were normalized to the total body activity.

MicroPET - FSall

Dynamic microPET scans were performed for 45min immediately after i.p. injection of 36MBq (0.98mCi) of [^{18}F]anginex in three mice. A two-dimensional OSEM image reconstruction was used. Images of data acquired from 6 to 45min are shown in Figure 4. Time-activity curves (Figure 5) were generated from regions of interest manually created over the tumor and reference tissue (muscle).

Conclusion

[^{18}F]Anginex was labeled in 76.8 \pm 3.5% chemical yield from [^{18}F]fluorobenzaldehyde. Preliminary microPET data show that uptake in two tumor types is substantial and selective, with a possibility of high tumor-to-background ratios. Further work to define the specificity of [^{18}F]anginex for its receptor gal-1 *in vivo* using PET imaging and biological correlate assays is ongoing in our laboratories and in feline head and neck clinical studies. Radiolabeled anginex is useful as a tracer for the development of therapeutic anginex and possibly as a general antiangiogenic diagnostic radiotracer.

The current work is a proof of principle that the biodistribution of [^{18}F]anginex and its uptake in tumors can be measured. This will allow detailed *in vivo* characterization of the targeting properties of anginex and exploration of potential applications for this nontoxic and stable peptide. Phase I/II trials of anginex are under way in felines with spontaneous head and neck tumors. It appears that the method established here for labeling anginex and imaging its tumor uptake may be a valuable addition to these comparative oncology studies to understand tumor targeting efficiency and the basic pharmacokinetic properties of this agent.

Acknowledgments

Supported by grant CA107160 and CA096090 from the NCI and by the Central Arkansas Radiation Therapy Institute.

References

- [1] P. Carmeliet, *Nature* 12-15-2005, 438, 932–936.
- [2] A. W. Griffioen, G. Molema, *Pharmacol. Rev.* 2000, 52, 237–268.

- [3] M. Amano, M. Suzuki, S. Andoh, H. Monzen, K. Terai, B. Williams, C. W. Song, K. H. Mayo, T. Hasegawa, R. P. Dings, R. J. Griffin, *Int. J. Clin. Oncol.* **2007**, *12*, 42–47.
- [4] M. M. Arroyo, K. H. Mayo, *Biochim. Biophys. Acta* **2007**, *1774*, 645–651.
- [5] J. Folkman, *Annu. Rev. Med.* **2006**, *57*, 1–18.
- [6] L. W. Dobrucki, A. J. Sinusas, *Curr. Opin. Biotechnol.* **2007**, *18*, 90–96.
- [7] R. Haubner, H. J. Wester, *Curr. Pharm. Des.* **2004**, *10*, 1439–1455.
- [8] X. Chen, R. Park, V. Khankaldyyan, I. Gonzales-Gomez, M. Tohme, R. A. Moats, J. R. Bading, W. E. Laug, P. S. Conti, *Mol. Imaging Biol.* **2006**, *8*, 9–15.
- [9] H. Wang, W. Cai, K. Chen, Z. B. Li, A. Kashefi, L. He, X. Chen, *Eur. J. Nucl. Med. Mol. Imaging* **2007**, *34*, 2001–2010.
- [10] B. Wagner, M. Anton, S. G. Nekolla, S. Reder, J. Henke, S. Seidl, R. Hegenloh, M. Miyagawa, R. Haubner, M. Schwaiger, F. M. Bengel, *J. Am. Coll. Cardiol.* **2006**, *48*, 2107–2115.
- [11] A. W. Griffioen, D. W. van der Schaft, A. F. Barendsz-Janson, A. Cox, H. A. Struijker Boudier, H. F. Hillen, K. H. Mayo, *Biochem. J.* **2001**, *354*, 233–242.
- [12] R. P. Dings, B. W. Williams, C. W. Song, A. W. Griffioen, K. H. Mayo, R. J. Griffin, *Int. J. Cancer* **2005**, *115*, 312–319.
- [13] R. P. Dings, D. W. van der Schaft, B. Hargittai, J. Haseman, A. W. Griffioen, K. H. Mayo, *Cancer Lett.* **2003**, *194*, 55–66.
- [14] R. P. Dings, Y. Yokoyama, S. Ramakrishnan, A. W. Griffioen, K. H. Mayo, *Cancer Res.* **2003**, *63*, 382–385.
- [15] D. W. van der Schaft, R. P. Dings, Q. G. de Lussanet, L. I. van Eijk, A. W. Nap, R. G. Beets-Tan, J. C. Bouma-Ter Steege, J. Wagstaff, K. H. Mayo, A. W. Griffioen, *FASEB J.* **2002**, *16*, 1991–1993.
- [16] R. P. Dings, M. Loren, H. Heun, E. McNeil, A. W. Griffioen, K. H. Mayo, R. J. Griffin, *Clin. Cancer Res.* **2007**, *13*, 3395–3402.
- [17] D. Jia, N. A. Koonce, R. Halakatti, X. Li, S. Yaccoby, F. L. Swain, L. J. Suva, L. Hennings, M. S. Berridge, S. M. Apana et al., *Radiat. Res.* **2010**, *173*, 809–817.
- [18] V. L. Thijssen, R. Postel, R. J. Brandwijk, R. P. Dings, I. Nesmelova, S. Satijn, N. Verhofstad, Y. Nakabeppu, L. G. Baum, J. Bakkers et al., *Proc. Natl. Acad. Sci. U.S.A.* **2006**, *103*, 15975–15980.
- [19] I. Camby, M. M. Le, F. Lefranc, R. Kiss, *Glycobiology* **2006**, *16*, 137R–157R.
- [20] M. Berridge, S. Apana, J. Hersh, *J. Labelled Compd. Radiopharm.* **2009**.
- [21] J. M. Beauregard, E. Croteau, N. Ahmed, J. E. van Lier, F. Benard, *J. Nucl. Med.* **2009**, *50*, 100–107.
- [22] J. W. Brodack, M. R. Kilbourn, M. J. Welch, J. A. Katzenellenbogen, *Int. J. Rad. Appl. Instrum. A* **1986**, *37*, 217–221.
- [23] Y. S. Ding, J. S. Fowler, S. J. Gatley, S. L. Dewey, A. P. Wolf, *J. Med. Chem.* **1991**, *34*, 767–771.
- [24] Y. S. Ding, J. S. Fowler, S. L. Dewey, J. Logan, D. J. Schlyer, S. J. Gatley, N. D. Volkow, P. T. King, A. P. Wolf, *J. Nucl. Med.* **1993**, *34*, 619–629.
- [25] Y. Y. Huang, W. S. Huang, T. C. Chu, C. Y. Shiue, *Appl. Radiat. Isot.* **2009**, *67*, 1063–1067.
- [26] W. J. McBride, R. M. Sharkey, H. Karacay, C. A. D'Souza, E. A. Rossi, P. Laverman, C. H. Chang, O. C. Boerman, D. M. Goldenberg, *J. Nucl. Med.* **2009**, *50*, 991–998.
- [27] B. Shen, W. Ehrlichmann, M. Uebele, H. J. Machulla, G. Reischl, *Appl. Radiat. Isot.* **2009**, *67*, 1650–1653.
- [28] C. Y. Shiue, J. S. Fowler, A. P. Wolf, M. Watanabe, C. D. Arnett, *J. Nucl. Med.* **1985**, *26*, 181–186.
- [29] E. M. van Oosten, A. A. Wilson, K. A. Stephenson, D. C. Mamo, B. G. Pollock, B. H. Mulsant, A. K. Yudin, S. Houle, N. Vasdev, *Appl. Radiat. Isot.* **2009**, *67*, 611–616.
- [30] J. Yoo, C. S. Dence, T. L. Sharp, J. A. Katzenellenbogen, M. J. Welch, *J. Med. Chem.* **2005**, *48*, 6366–6378.
- [31] M. S. Haka, M. R. Kilbourn, G. L. Watkins, S. A. Toorongian, *J. Lab. Compd. Radiopharm.* **1988**, *27*, 823–833.
- [32] X. Li, A. Pennisi, F. Zhan, J. R. Sawyer, J. D. Shaughnessy, S. Yaccoby, *Br. J. Haematol.* **2007**, *138*, 802–811.
- [33] K. Yata, S. Yaccoby, *Leukemia* **2004**, *18*, 1891–1897.